ELECTRONIC SUPPLEMENTARY INFORMATION

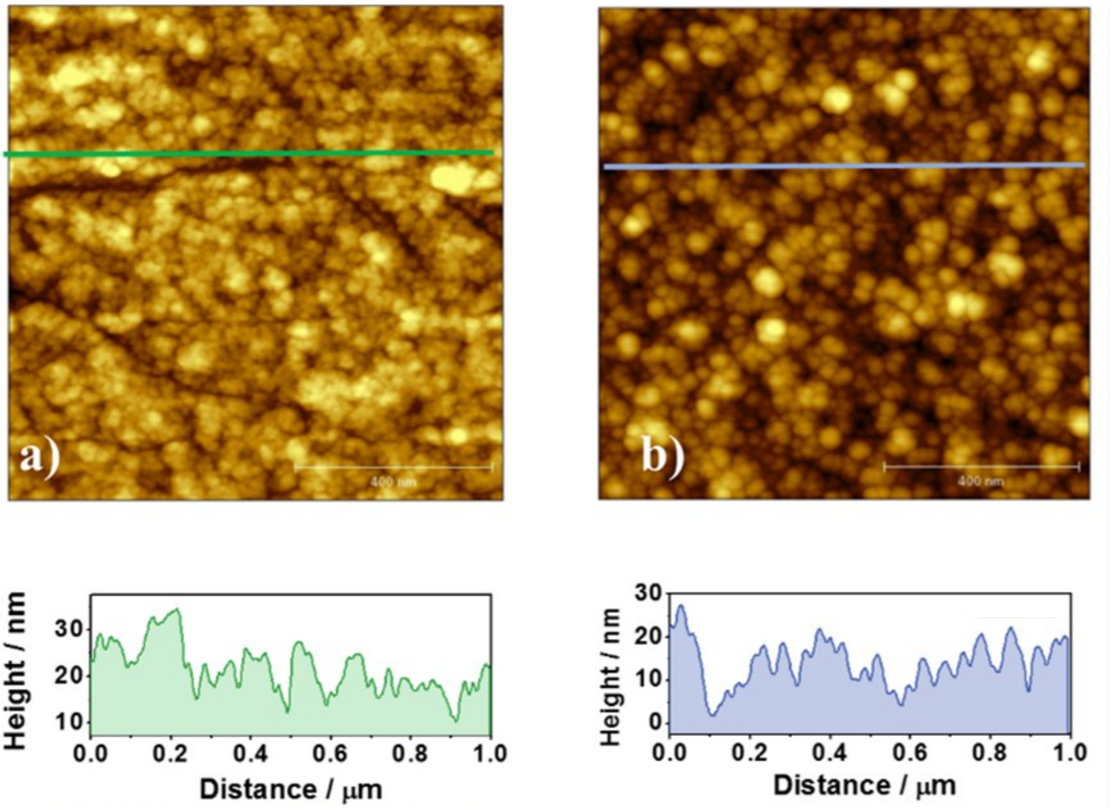

S1. AFM images (1 µm x 1 µm) corresponding to (a) NO_2 -M and (b) NH_2-M. Each image incorporates a representative cross section of the surface profile.

NO_2-M structure (Fig S1a) consists of globular particles homogeneously distributed that change their size after the reduction to NH_2 (Fig S1b). Thus, when the functional groups are mostly nitro species (Fig S1a) the particle size is around 23 +/- 10 nm and, as it can be seen, some HOPG step edges are still visible. On the other hand, the reduction step of NO_2 to NH_2 causes a notable increase in the particle size until 33 +/- 10 nm (Fig. S1b). This fact means that the reduction process of the multilayer is accompanied by noticeable changes in the morphology of the surface which cannot been understood as the simple reduction of the nitro groups to the amine ones. It seems clear that a deep reorganization of the inner structure of the film has taken place as a consequence of the reduction reaction.

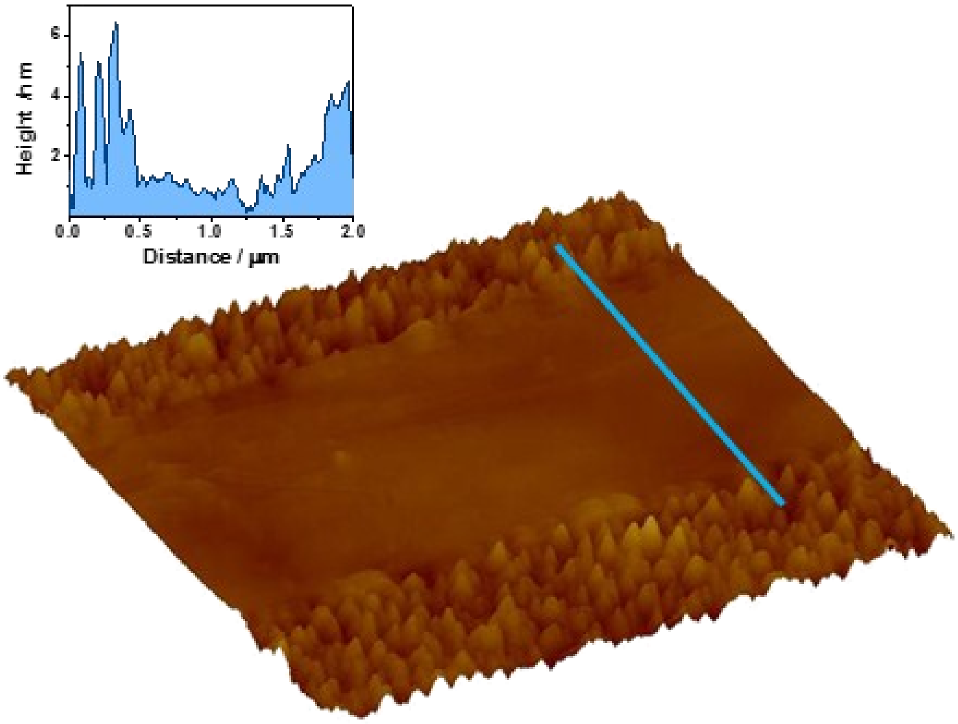

S2. AFM image (2.5 µm x 2.5 µm) showing the NO_2-M HOPG modified surface after scratching with the AFM tip and a representative cross section showing the multilayer thickness.

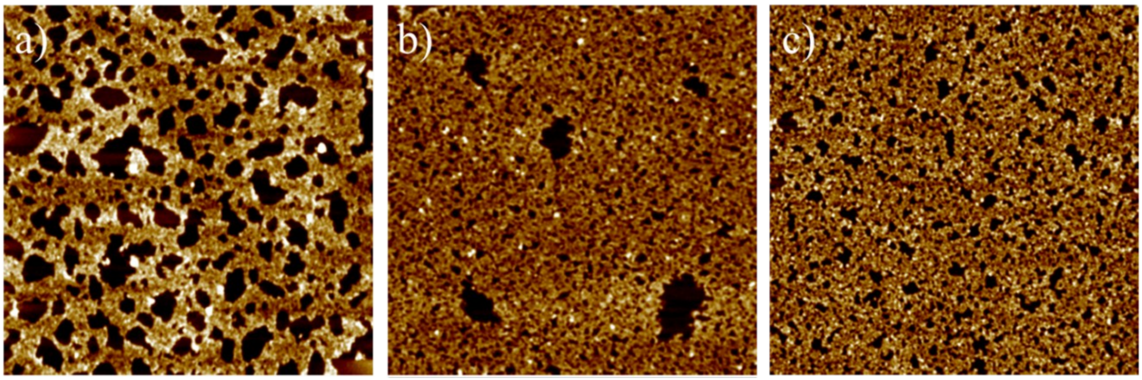

S3. AFM images (1 μm x 1 μm) for NO_2-m after a) 2 cycles; b) 4 cycles and c) 8 cycles on 1mM NBD + 2 mM DPPH in 0.1 M $TBABF_4$ showing how the monolayer grows.

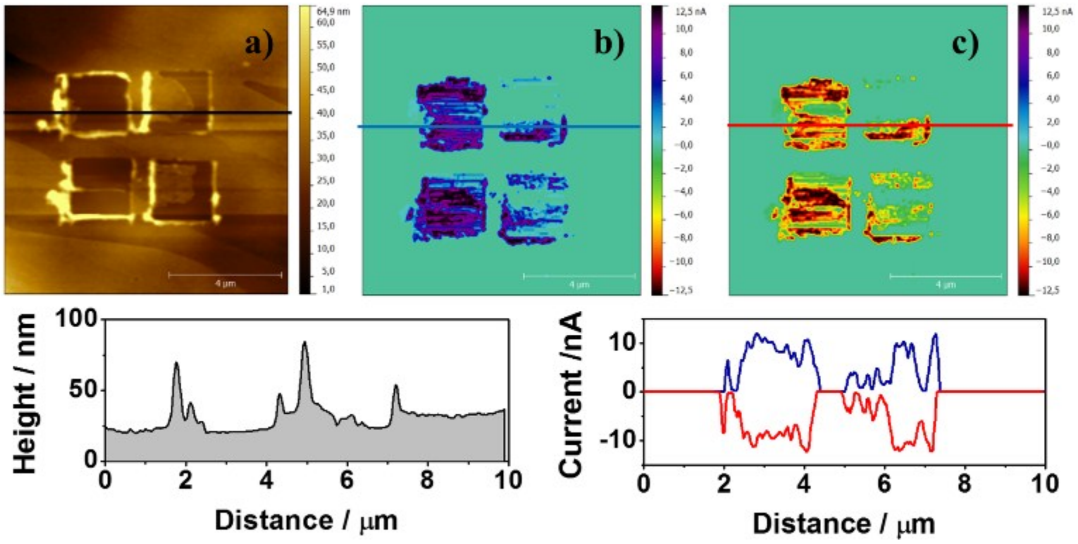

S4. (a) Topographic AFM image (10 µm x10 µm) and C-AFM images at (b) 0.5 V and (c) -0.5 V tip-sample applied potential for NO_2-M, and representative topographic and current cross sections. Note the zero current response out of the scratched areas in figures b and c.

In Figure S4a the topographic image of four squares carried out by scratching with the AFM tip to obtain uncovered areas showing the free substrate surface is shown. It is clear in the C-AFM images recorded at 0.5 V and -0.5 V (Fig S4b and S4c) that covered and uncovered areas have a very different electrical conductance.

While the free HOPG surface shows a response which perfectly follows the applied difference potential, the organic covered surface appears totally passivated after the functionalization with aryl diazonium salts. This can be observed as well in the cross sections shown in Figure S4b-c where changes in the sign of the current can be associated with that of the applied potential at the same time that topographic cross section is seen. It is important to take into account that especially low tip-loading force (less than 2nN) was chosen in these C-AFM measurements to avoid any damages on the film as a cause of working in AFM contact mode.

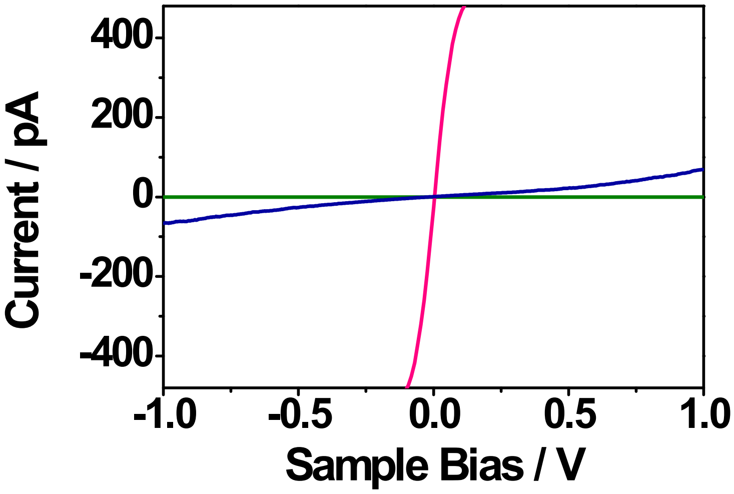

S5. Current-potential response obtained in C-AFM on free HOPG surface (red), NO_2-m surface (blue) and NO_2-M modified surface.

While free HOPG surface (red line) gives a very good conductive response, NO_2-m (blue line) exhibits certain conduction whereas NO_2-M (green line) appears as totally blocked between -1 and 1 V.

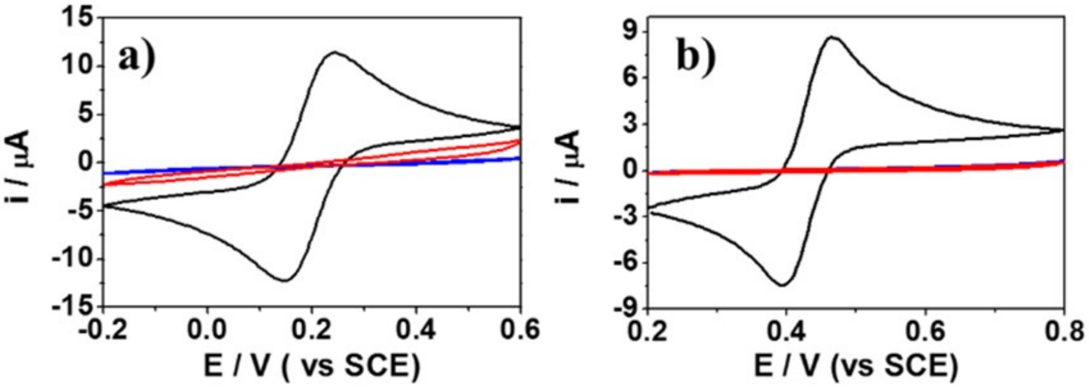

S6. Cyclic voltammograms showing the electrochemical response (black: HOPG; blue: NO_2; red: NH_2) (a) 1 mM $[Fe(CN)_6]^{4-}/[Fe(CN)_6]^{3-}$ + 0.1 M KNO_3 for multilayer films and (b) 1 mM dopamine + 0.01 M H_2SO_4 for multilayer films.

In the case of the multilayer (thickness around 6 nm) no significant electrochemical response is obtained in any case as can be seen in Figure S6a-b, although for NH_2-M there is a weak and irreversible response for the $Fe(CN)_6^{4-}$/ $Fe(CN)_6^{3-}$ system (Fig. S6a red line). This very small voltammetric current is likely related to some permeability in the layer of this redox probe favored by the lower hydrophobicity of the NH_2 layer with respect to the NO_2 one. On the other hand, in the case of dopamine (Fig. S6b) no voltammetric response is detected at all, a fact which confirms that the possible presence of pinholes or defects on the multilayer has a very low influence in the voltammetric response for the dopamine.

E_d / V	0.4	0	-0.4
Diameter / nm	103.5 ± 13.3	24.1 ± 5.9	8.6 ± 2.9
Height / nm	51.7 ± 9.2	15.1 ± 3.9	4.9 ± 1.5
Radii / nm	51.8 ± 6.6	12.1 ± 2.9	4.3 ± 1.4
(r/h) / nm	1 ± 0.1	0.85 ± 0.3	0.93 ± 0.3
Density / part µm^{-2}	6 ± 1	150 ± 20	940 ± 50

S7. Representative data obtained for gold electrodeposition on modified HOPG.

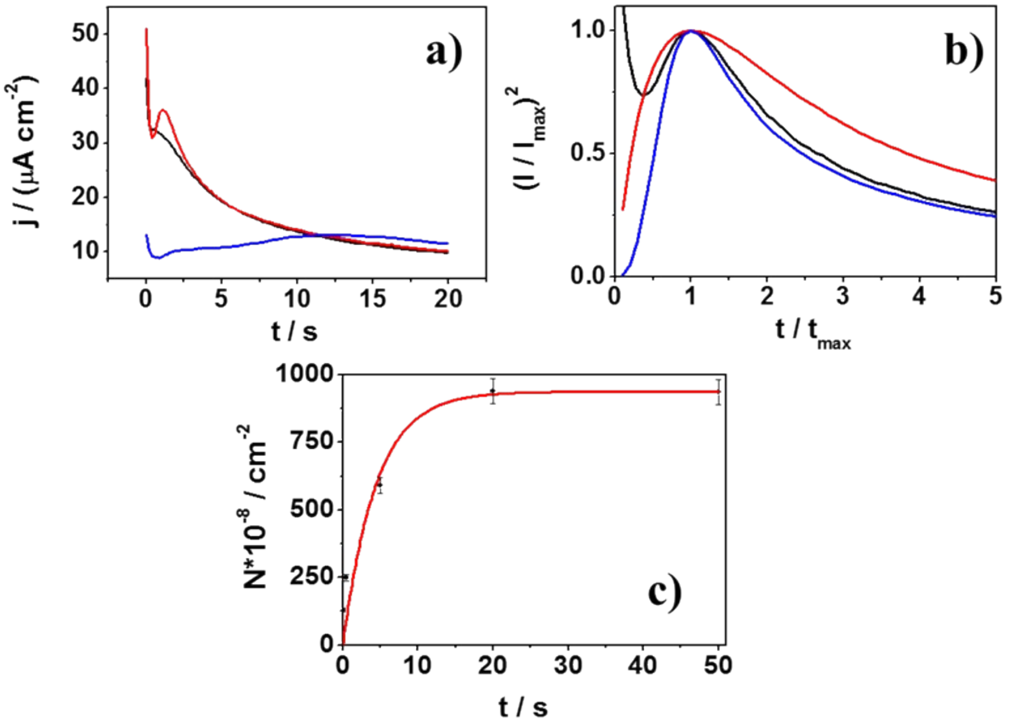

S8. (a) Different current-time transients for gold electrodeposition on a NH_2-m at E_d=0.42 V (blue), E_d=0.41 V (red) and E_d=0.40 V (black); (b)Theoretical $(i/i_{max})^2$ vs t/t_{max} curves predicted by Scharifker-Hills models for instantaneous (red) and progressive (blue) nucleation compared with the experimental data obtained at E_d=0.41 V (black); (c) Nuclei surface density vs electrodeposition time plot for gold nanoparticles grown at E_d =-0.4 V; red line corresponds to the equation indicated in the text.

The Scharifker-Hills model in the limiting cases of instantaneous and progressive nucleation and growth of 3D hemispherical particles can be tested by the following analytical expressions:

$$\frac{I^2}{I_m^2} = \frac{1.9542}{t/t_m}\left\{1 - exp\left[-1.2564\left(\frac{t}{t_m}\right)\right]\right\}^2$$ (Instantaneous nucleation)

$$\frac{I^2}{I_m^2} = \frac{1.2254}{t/t_m}\left\{1 - exp\left[-2.3367\left(\frac{t}{t_m}\right)^2\right]\right\}^2$$ (Progressive nucleation)

where i_m and t_m refer to the current and time of the maximum on the current-time transients.

Figure S8a shows three representative current-time transients obtained at different potentials for the gold electroreduction on the organic monolayer and their corresponding maximum for nucleation and growth, and Figure S8b shows the fix of the experimental data points for electroreduction potential E_d = 0.41 V. Our data (Fig S8b black line) seems to clearly follow the case of progressive nucleation which at the same time is fully consistent with the AFM images of Figure 7. Figure S8c shows the fit of the surface nuclei density as a function of the applied time for electroreduction potential E_d = -0.4 V.

	ΔE_p ($Fe(CN)_6^{4-}$/ $Fe(CN)_6^{3}$) / mV	**ΔE_p (Dopamine) / mV**
HOPG	97	68
NH_2-m	342	473
AuNPs (0.05s)	359	332
AuNPs (0.5s)	263	224
AuNPs (5s)	206	83
AuNPs (20s)	171	83

S9. Table with peak to peak potential separation corresponding to figures 4 a-b and 8 b-c. Potential separation error are less than ±10 mV.

As it can be seen, as the number of AuNPs grows a decrease in the ΔE_p and an increase in the peak current occurs.